Structure and Properties of Shape-Memory Polyurethane Block Copolymers

TOSHISADA TAKAHASHI,[1,*] NORIYA HAYASHI,[2] and SHUNICHI HAYASHI[2]

[1]Faculty of Engineering, Fukui University, Bunkyo 3-9-1, Fukui, Japan; and [2]Materials and Chemical Research Laboratory, Nagoya Research and Development Center, Mitsubishi Heavy Industries Ltd., Iwatsuka-Cho, Nakamae-Ku, Nagoya 453, Japan

SYNOPSIS

Segmented polyurethanes containing soft segments with lower molecular weight exhibit shape-memorizing properties. Structure and properties of shape-memorizing polyurethanes (S-PUs) were studied. S-PUs are characterized by a rather high glass transition temperature: T_g of S-PUs is usually in the range of 10–50°C. A plot of $1/T_m$ against $-\ln X_A$ is approximately linear, indicating that the hard segments are randomly distributed along the molecular chain. S-PUs with a hard segment of 67–80 mole % form negative spherulites; they give a faint scattering maximum in a small-angle X-ray diffraction pattern. On the other hand, S-PUs with a hard segment of 50 mole % form fine birefringent elements, giving diffuse scattering in its SAXD pattern. A cyclic test of an S-PUs above T_g indicates that the residual strain increases and the recovery strain decreases with increasing cycle and maximum strain. It has been suggested by dynamic mechanical investigation that the shape-memorizing property of the S-PUs may be ascribed to the molecular motion of the amorphous soft segments. © 1996 John Wiley & Sons, Inc.

INTRODUCTION

Segmented polyurethane (PU) is an important class of multiblock copolymers consisting of alternating sequences of hard and soft segments. A great deal of research on morphology,[1–14] crystal structure,[6–10] thermal behavior,[15–19] deformation behavior,[20,21] and rheological properties[22] of various kinds of PUs have been done in the field of segmented PU in the past decade. However, this polymer has been investigated mainly on its practical property as a rubber material.

Recently, it has been noticed that certain PUs exhibit interesting shape-memory properties.[23] Shape-memory PUs will hereafter be abbreviated "S-PUs". Usually S-PUs consist of polyester or polyether with a number average molecular weight of 300–1,000. These S-PUs are characterized by a rather high glass transition temperature (T_g); T_g of S-PUs is usually in the range of 10–50°C. S-PUs are set in a particular shape above T_g and cooled to a temperature below T_g; cooled S-PUs hold this particular shape as it is set. Heated to a temperature above T_g, the S-PUs return to their original shape.

This study is concerned mainly with the thermal, structural, and dynamic mechanical properties of the S-PUs. Two series of linear S-PUs based on poly(ethylene adipate) (PEA) glycol reacted with diphenylmethane diisocyanate (MDI) and extended with 1,4-butanediol (BDO) were used in this study. It has been suggested that the shape-memorizing property of the S-PUs may be ascribed to the molecular motion of the amorphous soft segments.

EXPERIMENTAL

Materials

S-PU samples used in this study were obtained from PEA, MDI, and BDO. Prepolymers were prepared by reacting MDI with PEA (M_w = ca. 300, ca. 600, ca. 1,000) at 60°C for 40 min. Synthesis was per-

* To whom correspondence should be addressed.

Journal of Applied Polymer Science, Vol. 60, 1061–1069 (1996)
 CCC 0021-8995/96/071061-09

formed with 5 mol % MDI excess. The resultant prepolymer was then extended with BDO at the same temperature. The S-PUs thus obtained were cast on a glass tray and cured at 120°C for 24 h. Mole ratios of MDI/BDO are shown in Table I.

Differential Scanning Calorimetry and Microscopy

Differential scanning calorimetry (DSC) was carried out over a temperature range from −40 to 250°C using a Seiko DSC-200. Runs were conducted at a heating rate of 20°C/min. Polarizing optical microscopy of sections was performed with an Olympus polarizing microscope (POM) equipped with an Olympus OM-N2 camera. Sections were cut with razor blade.

Wide-Angle and Small-Angle X-ray Diffractometry

Wide-angle X-ray diffraction (WAXD) traces were obtained in the transmission mode with a Rigaku-Denki X-ray diffractometer (D-1A) operated at 35 kV and 20 mA. WAXD studies were carried out with samples of 0.7 to 1.0 mm section thicknesses. Small-angle X-ray diffraction (SAXD) patterns were obtained using a Nihon-Denshi JRX-12VA diffractometer with a photographic attachment. In both cases, nickel-filtered CuKα radiation was used as the X-ray source.

Mechanical and Viscoelastic Properties

Measurements of the mechanical properties were carried out using a Shimadzu tensile tester (Autograph) equipped with a constant temperature chamber. Samples were elongated at a rate of 50%/min. Dynamic mechanical investigation was carried out using a Rheometrics viscoelastometer (RMS-800) in the temperature range from −30°C to 140°C. Shear strain of 0.05% was given with a working frequency of 1 Hz.

RESULTS AND DISCUSSIONS

Table I shows sample number, molecular weight of PEA, mole ratio of MDI/PEA/BDO, T_g, storage modulus (G'), and molecular weight of the two series of S-PUs used in this study. S-PUs of [A] series, [A]-S-PUs (PEA-2-3, 2-6, 2-10), consist of MDI; PEA with molecular weight of ca. 300, ca. 600, ca. 1,000; and BDO at the mole ratio of MDI/PEA/BDO = 2.1/1.0/1.0. S-PUs of [B] series, [B]-S-PUs (PEA-1-6, 2-6, 3-6, 4-6, 5-6), consist of MDI, PEA with molecular weight of ca. 600, and BDO at different MDI/PEA/BDO mole ratios. In the following, we discuss mainly the thermal properties, crystallinity, morphology, mechanical properties, and dynamic mechanical behavior of the [B] series of S-PUs.

Thermal Properties

DSC curves of [A]-S-PU with soft segments of varying length are shown in Figure 1(a). All samples show two or three transitions in the range from −25°C to 220°C. PEA-2-10, PEA-2-6, and PEA-2-3 exhibit a second-order transition at 4.8°C, 13°C, and 48.3°C, respectively. This second-order tran-

Table I Characterization of PU–PEA Block Copolymers Used in This Study

Sample Number	Mole Ratio[a]			M_w of PEA	T_g [°C][b] DYN/DSC	G' [Pa][c] at T_g + 20°C	Molecular Weight		
	MDI	PEA	1,4-BG				$M_w \times 10^5$	$M_n \times 10^5$	M_w/M_n
PEA-2-3	2.11	1.00	1.00	303	64/48.3	3.17×10^7	2.07	1.37	1.51
PEA-2-6	2.10	1.00	1.00	617	24/13.0	8.27×10^6	3.01	1.47	2.10
PEA-2-10	2.10	1.00	1.00	984	/−4.8	8.39×10^6	5.10	1.79	2.85
PEA-1-6	1.05	1.00	0	609	—/0.3	1.55×10^6	2.97	1.81	1.64
PEA-2-6	2.10	1.00	1.00	617	24/13.0	8.27×10^6	3.10	1.47	2.10
PEA-3-6	3.15	1.00	2.00	609	48/13.4	7.23×10^7	2.85	1.85	1.54
PEA-4-6	4.20	1.00	3.00	600	41/27.4	7.91×10^7	3.47	2.10	1.64
PEA-5-6	5.25	1.00	4.00	609	38/34.8	1.44×10^8	2.86	2.01	1.42

[a] Mole ratio (MDI: diphenyl methane diisocyanate; PEA: poly (ethylene adipate); 1,4-BG: 1,4-butene diole).
[b] T_g (DYN: dynamic measurement).
[c] G': dynamic modulus.

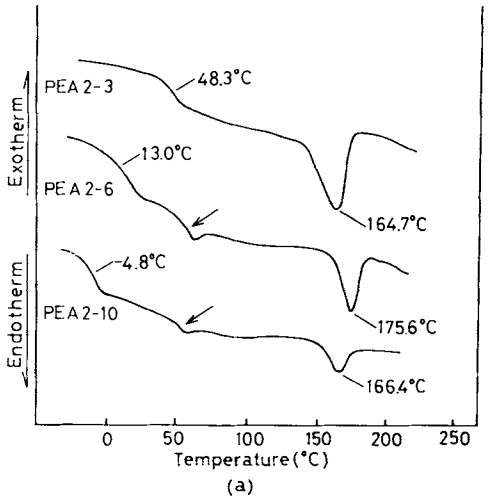

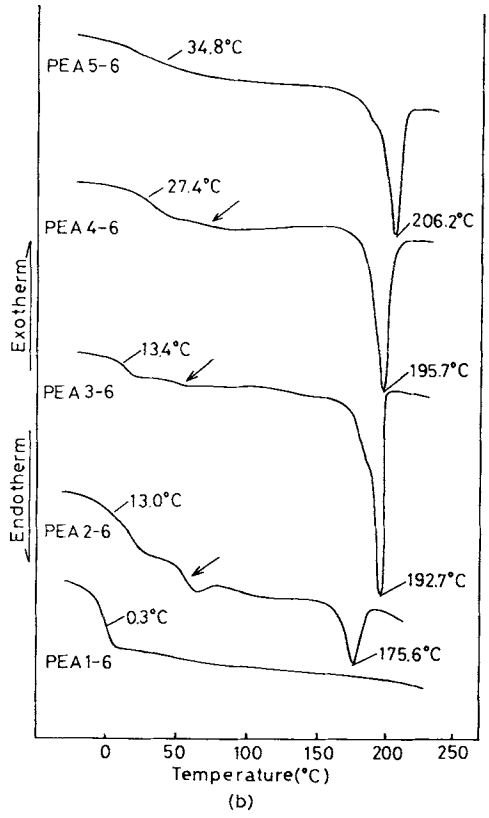

Figure 1 DSC curves for the heating of polyurethanes: (a) [A] series of polyurethanes; (b) [B] series of polyurethanes.

sition can be ascribed to the glass transition of the soft segment. As seen in Figure 1(a), T_g of [A]-S-PU is noticeably affected by the molecular weight of the soft segments; T_g decreases with an increase in the molecular weight of PEA. T_g of PEA-2-10 based on PEA with a molecular weight of 984 is −4.8°C. This T_g is still higher by 15°C than that of a PU elastomer based on PEA with a molecular weight of ca. 2,000.[14] An endotherm due to the melting of the soft-segment crystal was not detected in the DSC curves of [A]-S-PU.

The second transition is another second-order transition in the temperature interval of 55°C to 70°C, ascribed to the glass transition of the hard segment. As Figure 1(a) reveals, the temperature range of this transition is little affected by the molecular weight of the soft segment and is the same as that of the PU elastomer.[14] This transition in sample PEA-2-3 is very weak, so the hard segment in the amorphous state is not great. The last transition is an endotherm at 160–205°C due to the melting of hard-segment crystals.

DSC curves of [B]-S-PU based on PEA (M_w = ca. 600) with varying MDI/PEA/BDO ratios are shown in Figure 1(b). As seen here, T_g of the soft segment shifts to higher temperature as the hard-segment content increases. It seems reasonable to assume that the mobility of the soft segments is restricted by the hard segment to which the soft segments are linked. Another effect of the hard segment is confirmed by the fact that the jump in heat capacity accompanying the glass transition of soft segments becomes lower as the hard-segment content increases. On the other hand, the glass transition of the hard segments of [B]-S-PU is not dependent on the hard-segment content.

The melting point of [B]-S-PU moves to lower temperatures as the hard-segment content decreases [Fig. 1(b)]. Melting point depression in random copolymer can be predicted by using a theory developed by Flory.[24] In the present study, the reciprocal of the melting temperature ($1/T_m$) was plotted as a function of $-\ln X_A$ (mole fraction of hard segment). The result is shown in Figure 2. A plot of $1/T_m$ against $-\ln X_A$ is approximately linear, indicating that the hard segments are randomly distributed along the molecular chain of the S-PUs used in this study. An extrapolation of $1/T_m$ against $-\ln X_A$ to the ordinate gives $1/T_m$, a reciprocal of the equilibrium melting point of the hard segment. T_m can be estimated at 219.7°C.

Morphology

Morphology of [B]-S-PU was studied using POM. Figure 3 comprises four POM micrographs of sample sections taken with crossed polarizers. The systematic changes in the [B]-S-PUs have been observed.

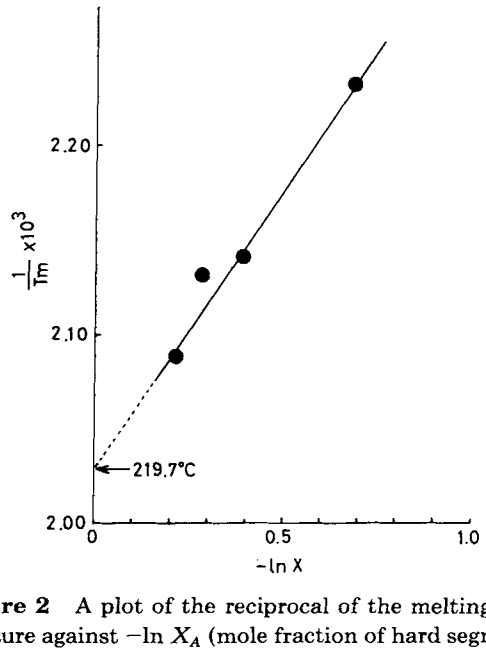

Figure 2 A plot of the reciprocal of the melting temperature against $-\ln X_A$ (mole fraction of hard segment).

Figure 3(a) is a POM micrograph of PEA-5-6 with the hard segment content of 80 mol %, showing that the well-developed spherulites with a diameter of approximately 30–100 μm fill the whole area of the POM micrographs. Fibrillar crystals are radially arranged into the spherulites. These spherulites are obviously formed from the hard segments.

Polarizing optical microscopy indicates that these spherulites are optically negative. The optical property of the spherulite is explained by assuming that the molecular axis orients perpendicular to the long axis of the fibrillar crystal. As shown in Figure 3(b), PEA-4-6 showed a morphology similar to that of PEA-5-6.

Figure 3(c) is a POM micrograph of PEA-3-6 with the hard segment content of 67 mol %. Almost the whole area is covered with smaller spherulites and birefringent elements. No distinct Maltese cross is observed, suggesting that the fibrillar crystals are irregularly arranged in these spherulites.

Figure 3(d) is a POM micrograph of PEA-2-6 with 50 mol % of hard segment, revealing very small birefringent elements. The spherulitic structures are no longer observed in the POM micrograph. A higher content of the soft segments in this sample is the reason why the characteristic spherulites are not formed. In fact, as the WAXD pattern of PEA-2-6 shows, the crystallinity of PU-2-6 is very low compared to PEA-3-6, PEA-4-6, and PEA-5-6. In this series of S-PUs, there is no evidence of soft-segment crystallization.

The morphology of MDI/PEA/BDO PUs with differing hard segment contents was studied by Foks and coworkers.[12–14] These PUs contain PEA with a molecular weight of ca. 2,000. The morphology of PUs and S-PUs with the same MDI/PEA/BDO mole ratios has been compared. For example, a POM micrograph of PU(MDI/PEA/BDO = 4/1/3) shows that small spherulites, approximately 5 μm in diameter, are dispersed in the amorphous matrix that occupies 70% or more of the whole area.[13]

The mole ratio of this PU sample corresponds to that of S-PU PEA-4-6. Obviously the size of the PU spherulites is significantly smaller than that of PEA-4-6. Furthermore, an amorphous matrix is not observed in the POM micrograph of PEA-4-6 [Fig. 3(b)]. These differences in morphology between PUs and S-PUs reflect the difference in the molecular weight of the soft segment. It is reasonable to assume that the longer PEA segments interfere with the crystallization of hard segments.

WAXD

Unoriented S-PU samples cured at 120°C were analyzed using a WAXD. Figure 4 shows the WAXD patterns for [B]-S-PU. Although PEA-2-6 exhibits a hard-segment melting peak at 175.6°C, it does not give distinct crystalline reflections in the WAXD pattern because of its low hard segment order; crystalline reflections are merged into the amorphous halo. The crystallinity of the hard segment increases with hard-segment fraction. As seen in Figure 4, PEA-3-6, PEA-4-6, and PEA-5-6 give a shoulder at 0.49 nm and some broad peaks at 0.46, 0.41, and 0.37 nm. The strongest crystalline reflection is the 0.45 nm line ($2\theta = 19.5°$).

The crystal structure of PU hard segment has been studied by Born and colleagues,[27] Briber and Thomas,[1,4] Blackwell and Lee,[2,3] and Quay and coworkers.[5] It has been reported that MDI/BDO-based PUs crystallize into three distinct crystal structures: types I, II, and III. Unoriented PU exhibits a type-II structure with a contracted conformation (monomer repeat unit of 1.72 nm), whereas oriented PU exhibits a type-III structure with a fully extended conformation (monomer repeat unit of 1.90 nm). According to Briber, the prominent d-spacings of the type-II structure are 0.490, 0.462, 0.445, 0.412, 0.377, 0.349, and 0.86 nm; the reflection at 0.86 nm corresponds to the (002) plane.[5]

WAXD patterns of unoriented MDI/BDO-based S-PUs can be explained on the basis of the type-II

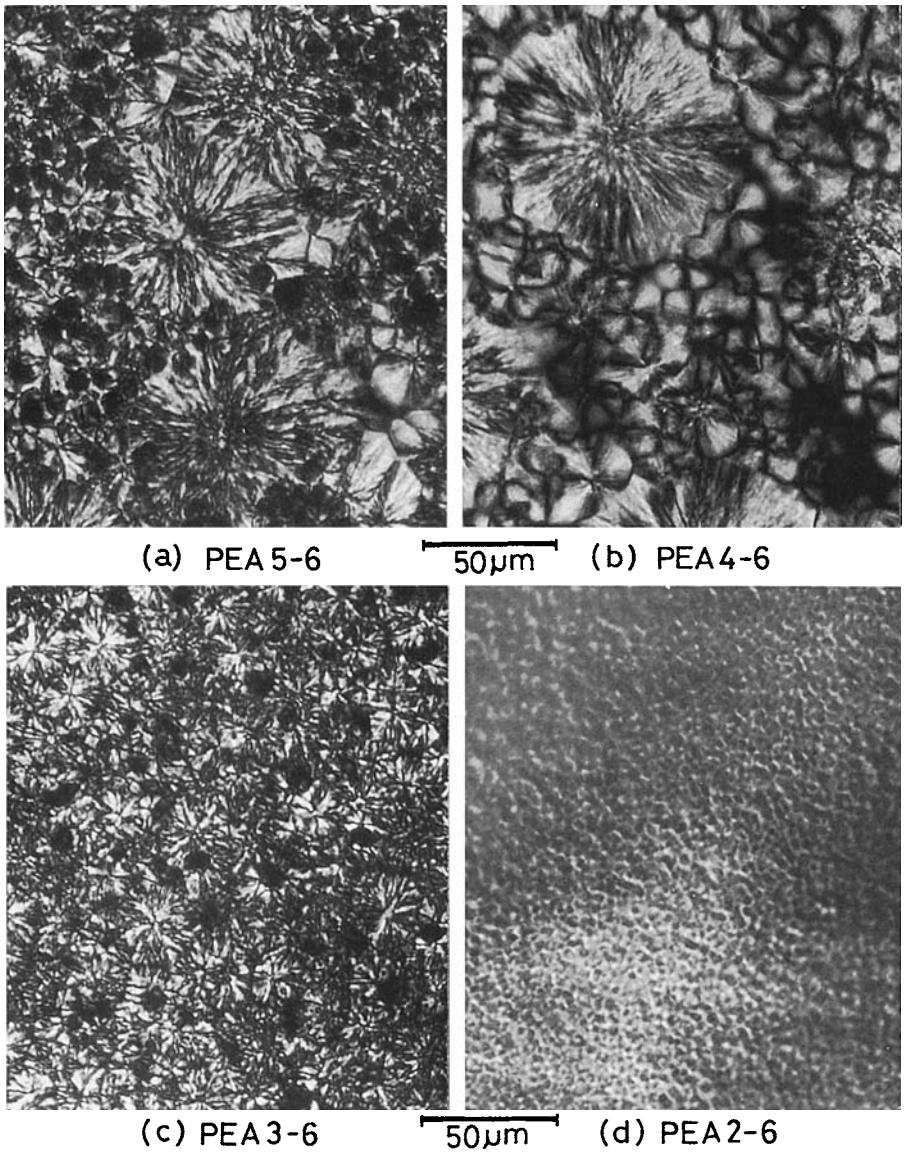

Figure 3 Polarizing optical micrographs of [B] series of polyurethanes.

structure. It seems that weak reflections at 0.86, 0.445, and 0.349 nm are merged into the background.

SAXD

SAXD was used to examine the supermolecular structure of S-PUs. SAXD patterns of some [B]-S-PU are shown in Figure 5. PEA-5-6, PEA-4-6, and PEA-3-6 give faint Bragg-type maxima in the SAXD patterns. The long spacing of PEA-5-6 calculated from a SAXD pattern is 13.7 nm, whereas the long spacing of PEA-4-6 is 15.7 nm. It is reasonable to assume that the long period of S-PUs is expanded by PEA segments that might exist in the amorphous region between the stacked lamellar crystals of the hard segment. Similar phenomena were observed in some block copolymers such as nylon-12/poly(propylene oxide)[25] and poly(hexamethylene *p,p'*-bibenzoate)/poly(tetramethylene oxide).[26]

The long spacing of PEA-3-6 is about the same as that of PEA-4-6; the Bragg-type maximum becomes fainter. This result suggests that amorphous PEA segments exist not only in the amorphous region between lamellar crystals of the hard segment but also in the amorphous matrix. On the other hand, PEA-2-6 gives only a diffuse scattering in the SAXD pattern, suggesting that fine crystallites of

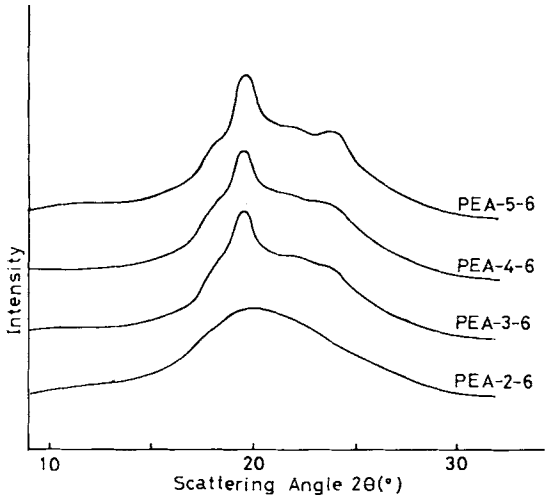

Figure 4 Wide-angle X-ray diffraction patterns of [B] series of polyurethanes.

the hard segment are dispersed in the amorphous matrix. These results are consistent with those of WAXD and POM studies.

Mechanical Properties

Stress–strain curves of [B]-S-PUs were recorded at a temperature of [T_g + 20] °C up to 300% of strain. Although the results are not included in this paper, the mechanical properties of [B]-S-PUs determined by the stress–strain analysis have shown a wide range of behavior with changes to the hard-segment content. The stress–strain curves of PEA-5-6, PEA-4-6, and PEA-3-6 have a gentle yield point at 150–200% of elongation, whereas PEA-2-6 does not give a clear yield point. The initial modulus and the stress level during deformation increase with increasing hard segment content. The mechanical behavior of S-PU can be explained on the basis of alternation in the overall crystallinity of the samples.

Cyclic tensile tests of some S-PUs are now in progress. The results of these tests will be discussed in connection with the shape-memorizing of the S-PU. In this paper, we demonstrate only an example of the cyclic test of PEA-4-6. The loading–unloading cycles were repeated 10 times at [T_g + 20] °C. In each cycle, stress was applied 5 min after unloading. The results are shown in Figures 6(a) and 6(b), in which the maximum strain is 20% and 100%, respectively.

Figure 6 indicates that the residual strain increases and the recovery strain decreases with increasing cycle and maximum strain. These results may be attributed to the plastic deformation of the hard-segment crystal or the flow of amorphous seg-

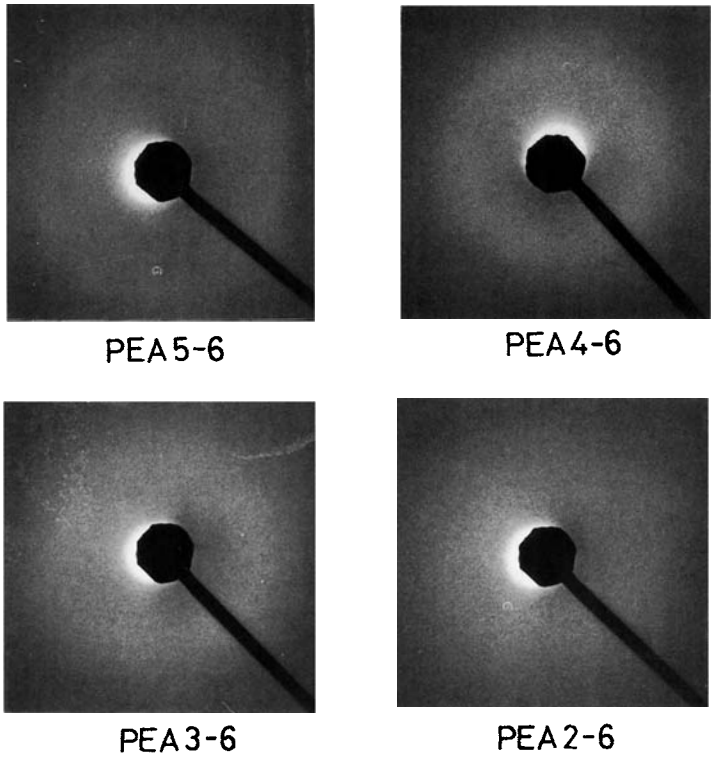

Figure 5 Small-angle X-ray diffraction patterns of [B] series of polyurethanes.

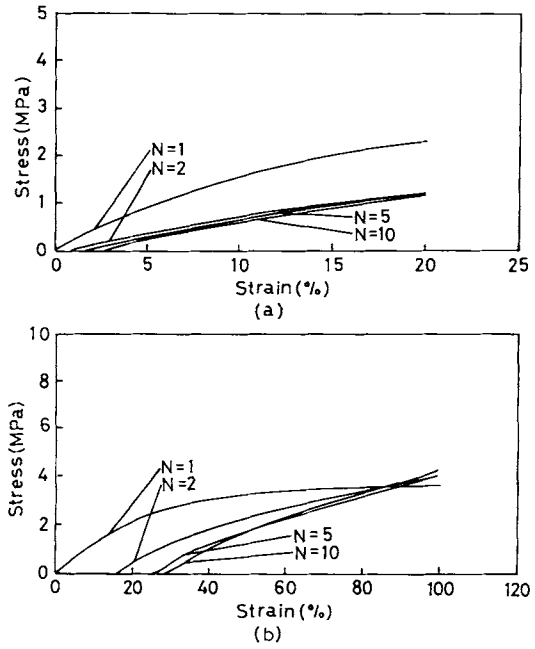

Figure 6 Cyclic tensile test of PEA-4-6. The loading–unloading cycles were repeated 10 times at $[T_g + 20]$°C.

ments. It seems reasonable to assume that the breaking of hydrogen bonds between molecular chains followed by the flow of amorphous segments plays an important role in the plastic deformation of PEA-2-6, since the crystallinity of PEA-2-6 is appreciably lower.

Dynamic Mechanical Properties

Dynamic mechanical investigations have been made in the temperature range of −30°C to 140°C. The storage modulus G' and the dissipation factor, tan δ, of [A]-S-PU are plotted as a function of temperature in Figure 7. Correspondingly, the storage modulus of [A]-S-PUs begins to fall at 45, 0, and −20°C for the samples of PEA-2-3, 2-6, and 2-10. Comparing Figure 7 with Figure 1(a), the fall in G' may be related to the glass transition of soft segments.

As is obvious from Figure 7(b), the location of loss peak is strongly dependent on the molecular weight of PEA. As the molecular weight of PEA increases, this transition shifts to higher temperatures; whereas the peak intensity remains constant. This transition is attributed to the backbone motion of the soft segments. It may be noted that the backbone motion of soft segments is affected by the "span" length of the PEA segment; both of the chain ends of PEA are linked to the hard segment.

The storage modulus G' and the tan δ of [B]-S-PU are plotted as a function of temperature in Figure 7. G' falls remarkably at the temperature range of 10–30°C depending upon the MDI/PEA/BDO mole ratio. The intensity and location of the loss peak at lower temperatures are dependent on the MDI/PEA/BDO mole ratio. As the hard segment increases, loss peak tends to shift to higher temperatures while the peak intensity becomes lower and broader. As is obvious from DSC scans in Figure 1(b), the fall in G' and the location of the loss peak of [B]-S-PU can be related to the glass transition of the soft segment.

The curves of tan δ for PEA-3-6 and PEA-4-6 reveal a second loss peak at 50°C; the second loss peak for PEA-5-6 is superimposed upon the first one. The location of the second loss peak is little affected by the MDI/PEA/BDO mole ratio. As DSC curves for these samples indicate, these second loss peaks can reasonably be associated to the glass transition of the hard segments.

CONCLUSIONS

Structure and properties of S-PUs were studied using POM, DSC, WAXD, SAXD, a tensile tester, and a viscoelastometer. Two series of linear S-PUs based on PEA, reacted with MDI, and extended with BDO were used in this study. The following results were obtained.

1. T_gs of S-PUs are noticeably affected by the molecular weight of the soft segment and MDI/PEA/BDO mole ratio. S-PUs are characterized by a rather high T_g: usually in the range of 10–50°C.
2. A plot of the reciprocal of T_m against $-\ln X_A$ is approximately linear, indicating that the hard segments are randomly distributed along the molecular chain of the S-PU.
3. S-PUs with hard segment contents of 75–80 mole % form well-developed negative spherulites, whereas S-PU with 50 mole % hard segments form very small birefringent elements.
4. S-PUs with the hard segment of 67–80 mole % give a scattering maximum in the SAXD pattern, whereas S-PUs with the hard segment of 50% give only a diffuse scattering in their SAXD patterns.

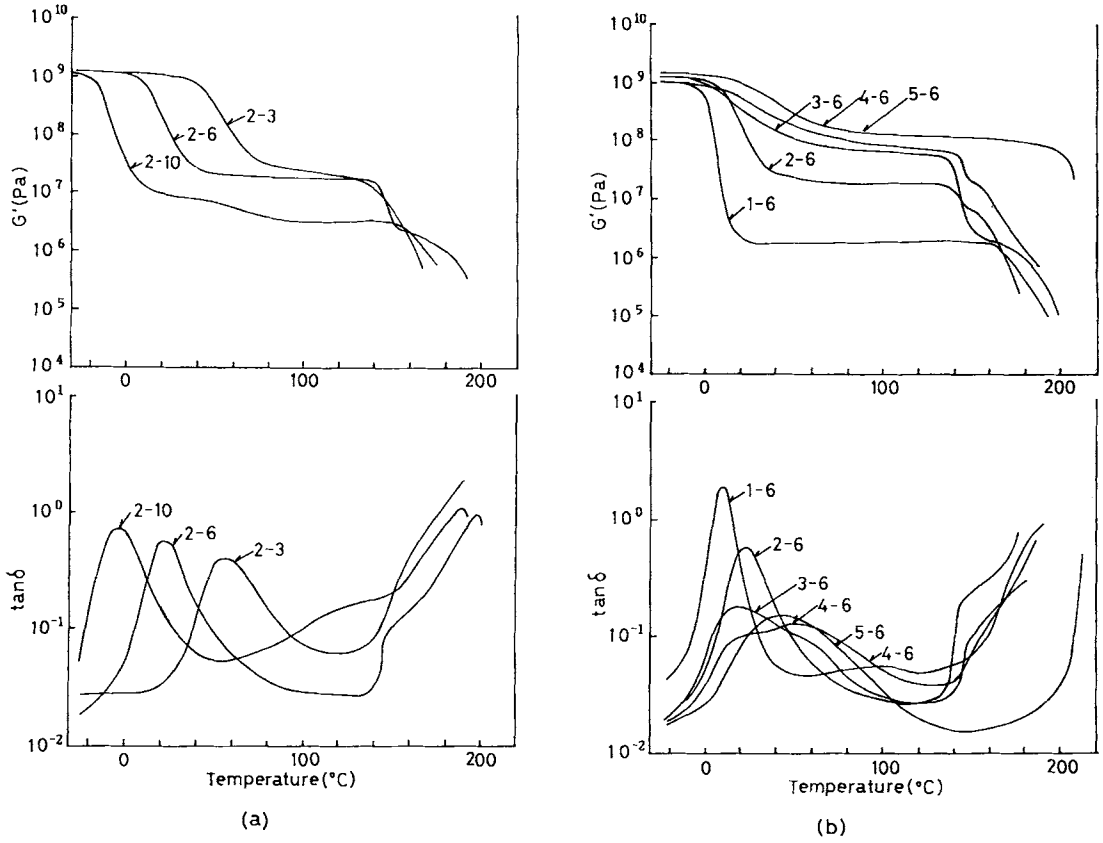

Figure 7 The storage modulus, G', and the dissipation factor, tan δ, of segmented polyurethanes: (a) [A] series of polyurethanes; (b) [B] series of polyurethanes.

5. Cyclic test of S-PU with the hard segment of 75 mole % indicate that the residual strain increases and the recovery strain decreases with increasing cycle and maximum strain.
6. Dynamic mechanical investigations indicate that the shape-memorizing properties of S-PUs can be ascribed to the molecular motion of the amorphous soft segments.

REFERENCES

1. R. M. Briber and E. L. Thomas, *J. Macromol. Sci., Phys.*, **B22,** 509 (1983).
2. J. Blackwell and C. D. Lee, *J. Polym. Sci., Polym. Phys. Ed.*, **21,** 2169 (1983).
3. J. Blackwell and C. D. Lee, *J. Polym. Sci., Polym. Phys. Ed.*, **22,** 759 (1984).
4. R. B. Briber and E. L. Thomas, *J. Polym. Sci., Polym. Phys. Ed.*, **23,** 1915 (1985).
5. J. R. Quay, Z. Sun, J. Blackwell, R. M. Briber, and E. L. Thomas, *Polym. J.*, **31,** 1003 (1990).
6. W. Neumuller and R. Bonarat, *J. Macromol. Sci., Phys.*, **B21,** 203 (1982).
7. J. Koberstein and R. S. Stein, *J. Polym. Sci., Polym. Phys. Ed.*, **21,** 1439 (1983).
8. J. Koberstein and T. P. Russell, *Macromolecules,* **19,** 714 (1986).
9. H. Meyer and R. Bonart, *Progr. Colloid Polym. Sci.*, **71,** 103 (1985).
10. P. E. Gibson, J. W. van Bonart, and S. L. Cooper, *J. Polym. Sci., Part B, Polym. Phys.*, **24,** 885 (1986).
11. J. Foks and G. Michler, *J. Appl. Polym. Sci.*, **31,** 1281 (1986).
12. J. Foks and H. Janik, *Polym. Eng. Sci.*, **29,** 113 (1989).
13. J. Foks, H. Janik, R. Russo, and S. Winiecki, *Eur. Polym. J.*, **25,** 31 (1989).
14. J. Foks, H. Janik, and R. Russo, *Eur. Polym. J.*, **26,** 309 (1990).
15. T. R. Hesketh, J. W. C. van Bogart, and S. L. Cooper, *Polym. Eng. Sci.*, **20,** 190 (1980).

16. E. J. Woo, G. Farber, R. J. Farris, C. P. Lillya, and J. C. W. Chien, *Polym. Eng. Sci.*, **25,** 834 (1985).
17. M. E. Kazmierczak, R. E. Fornes, D. R. Buchanan, and R. D. Gilbert, *J. Polym. Sci., Part B, Polym. Phys.*, **27,** 2173 (1989).
18. M. E. Kazmierczak, R. E. Fornes, D. R. Buchanan, and R. D. Gilbert, *J. Polym. Sci., Part B, Polym. Phys.*, **27,** 2189 (1989).
19. J. T. Koberstein and A. F. Galambos, *Macromolecules*, **25,** 5618 (1992).
20. H. Ishihara, I. Kimura, and N. Yoshihara, *J. Macromol. Sci., Phys.*, **B22,** 713 (1983–84).
21. H. Ishihara, *J. Macromol. Sci., Phys.*, **B22,** 763 (1983–84).
22. G. Spathis, E. Kontou, V. Kefalas, L. Apekis, C. Christodoulides, and P. Pissis, *J. Macromol. Sci., Phys.*, **B29,** 31 (1990).
23. S. Hayashi, S. Kondo, and K. Kawamura, *34th Annual Polyurethanes Technical/Marketing Conf.*, 1992, p. 605.
24. P. J. Flory, *Trans. Faraday Soc.*, **51,** 848 (1955).
25. T. Shikata, N. Hayashi, T. Sasaki, and T. Takahashi, *Polym. Prepr., Japan*, 20R-21 (1993).
26. T. Takahashi and F. Nagata, *J. Macromol. Sci., Phys.*, **B30,** 2581 (1992).
27. L. Born, J. Crone, H. Hespe, and K. H. Wolf, *Colloid Polym. Sci.*, **260,** 819 (1982).

Received April 19, 1994
Accepted July 29, 1995